Published in final edited form as:
J Neurosci. 2008 May 21; 28(21): 5460–5464. doi:10.1523/JNEUROSCI.0257-08.2008.

Aquaporin-4 Deficient Mice have Increased Extracellular Space Without Tortuosity Change

Xiaoming Yao[1,2], **Sabina Hrabětová**[3,4], **Charles Nicholson**[3], and **Geoffrey T. Manley**[1,2]

1*University of California, San Francisco, Dept. of Neurosurgery*

2*University of California, San Francisco, Brain and Spinal Injury Center*

3*New York University School of Medicine, Dept. of Physiology and Neuroscience*

4*State University of New York, Downstate Medical Center, Dept. of Anatomy and Cell Biology*

Abstract

Aquaporin-4 (AQP4) is the major water channel expressed at fluid-tissue barriers throughout the brain and plays a crucial role in cerebral water balance. To assess whether these channels influence brain extracellular space (ECS) under resting physiological conditions, we used the established real-time iontophoresis method with tetramethylammonium (TMA^+) to measure three diffusion parameters: ECS volume fraction (α), tortuosity (λ), and TMA^+ loss (k'). *In vivo* measurements were performed in the somatosensory cortex of AQP4 deficient ($AQP4^{-/-}$) mice and wild-type controls with matched age. Mice lacking AQP4 showed a 28% increase in α (0.23 ± 0.007 vs. 0.18 ± 0.003) with no differences in λ (1.62 ± 0.04 vs. 1.61 ± 0.02) and k' (0.0045 ± 0.0001 1/sec vs. 0.0031 ± 0.0009 1/sec). Additional recordings in brain slices showed similarly elevated α in $AQP4^{-/-}$ mice, and no differences in λ and k' between the two genotypes. This is the first direct comparison of ECS properties in adult mice lacking AQP4 water channels with wild-type animals and demonstrates a significant enlargement of the volume fraction but no difference in hindrance to TMA^+ diffusion, expressed as tortuosity. These findings provide direct evidence for involvement of AQP4 in modulation of the ECS volume fraction and provide a basis for future modeling of water and ion transport in the central nervous system.

Keywords

Aquaporin-4; diffusion; tetramethylammonium; volume fraction; seizure; water transport

INTRODUCTION

Aquaporin-4 (AQP4) is the major membrane water channel in the central nervous system. AQP4 is expressed in astrocyte foot processes in direct contact with capillary vessels in the brain (Frigeri et al., 1995 and Nielsen et al., 1997). AQP4 is also expressed in the astrocytic processes that form the glia limitans, a structure adjacent to the cerebrospinal fluid-filled subarachnoid space and ventricles. Expression of AQP4 at these tissue-fluid interfaces indicates a role in maintaining brain water homeostasis. Phenotype studies of transgenic mice lacking AQP4 demonstrate its involvement in cerebral water balance and neural signal transduction (Manley et al., 2004). $AQP4^{-/-}$ mice have an increased seizure threshold (Binder

Address correspondence to: Geoffrey T. Manley, M.D., Ph.D., Associate Professor, Department of Neurological Surgery, University of California, San Francisco, 1001 Potrero Avenue, Room 101, San Francisco, CA 94110, Phone: (415) 206-4536, Fax: (415) 206-4466, E-mail: manley@itsa.ucsf.edu.

et al., 2004b) and prolonged seizure duration with slowed K^+ kinetics in the brain extracellular space (ECS) (Binder et al., 2006). α-syntrophin-deficient mice, where AQP4 is not properly targeted to the cell membrane, also show the deficit in K^+ clearance (Amiry-Moghaddam et al., 2003). These observations might be explained if ECS volume fraction α (defined as the ratio of ECS volume to that of whole tissue) were increased by AQP4 deletion (Manley et al., 2004) delaying the accumulation and clearance of neuroactive substances in the ECS. After birth, α is about 0.4 in rodent neocortex (Lehmenkühler et al 1993) and shrinks to about 0.2 in the adult with a time-course that matches glial proliferation and AQP4 expression (Wen et al. 1999). Consequently, it might be hypothesized that, in the absence of AQP4, this contraction of the ECS does not occur. Indeed, it has been claimed that the effective diffusion coefficient of dextran macromolecules increases in $AQP4^{-/-}$ mice (Binder et al. 2004a, Papadopoulos and Verkman 2005, Zador et al. 2008), which these authors interpreted as implying an increase in α. It was important, therefore, to directly test the hypothesis that α is enlarged in $AQP4^{-/-}$ mice and to obtain an absolute value for this and other diffusion parameters that might affect the role of AQP4 in brain water movement.

We used the real-time iontophoresis method with tetramethylammonium (RTI-TMA method; Nicholson & Phillips 1981) to measure α and tortuosity λ (defined as $(D/D^*)^{1/2}$ where D is the free diffusion coefficient of TMA^+ and D^* is the effective diffusion coefficient in brain) in $AQP4^{-/-}$ and $AQP4^{+/+}$ mice both *in vivo* and *in vitro*. We found a significant increase in ECS volume fraction in AQP4-deficient mice with no change in tortuosity. These findings are discussed in the context of seizure threshold and provide a basis for future modeling of water and ion transport.

MATERIALS AND METHODS

In vivo experiments took place at the University of California, San Francisco under a Committee on Animal Research (CAR) approved protocol. *In vitro* experiments were performed at New York University School of Medicine in conformity with local Institutional Animal Care and Use Committee (IACUC) regulations.

Mice

$AQP4^{-/-}$ mice were generated in a CD1 genetic background (Ma et al., 1997). These mice lack detectable AQP4 protein and phenotypically had normal growth, development, survival, and neuromuscular function. Brains from wild type and $AQP4^{-/-}$ mice showed no gross anatomical differences (Manley et al., 2000). Male $AQP4^{+/+}$ and $AQP4^{-/-}$ mice were used with matched age and body weight (3-4 months, 30-35 g for the *in vivo* study and 4-4.5 months, 35-46 g for the *in vitro*). Twenty mice were used: seven $AQP4^{+/+}$ and seven $AQP4^{-/-}$ for *in vivo* studies and three $AQP4^{+/+}$ and three $AQP4^{-/-}$ mice for *in vitro*.

In vivo *animal preparation*

Mice were anesthetized using 2.5% Avertin (2,2,2-tribromoethanol, 250 mg/kg, i. p., Sigma-Aldrich, St. Louis, MO) and immobilized in a stereotaxic apparatus. An additional 85 mg/kg Avertin was given every hour to maintain anaesthesia. After exposing the skull by midline skin incision, an atraumatic craniectomy was made over the somatosensory cortex (1.5 mm lateral and 1.5 mm caudal to bregma) using a micro drill and the dura was carefully removed. The skin flaps were held open with a cylindrical plastic dam (13 mm diameter and 4 mm height; Fig. 1A) and artificial cerebrospinal fluid (ACSF; see below), at 37°C, superfused over the brain at 2 ml/min. A small plastic container (4 mm diameter and 5 mm height) was glued to the inner wall of the dam to hold agarose gel for control measurements. The mice breathed room air spontaneously and a heating pad maintained body temperature at 37 ± 0.5°C. Measurements were made at 1-3 hours after surgery. The ACSF composition was (in mM):

126 NaCl, 3 KCl, 26 $NaHCO_3$, 1.25 NaH_2PO_4, 10 D-glucose, 1.3 $MgCl_2$, 1.5 $CaCl_2$, gassed with 95% O_2/5% CO_2 to buffer pH at 7.4. For TMA^+ calibration, 0.5 mM TMA-chloride was added.

In vitro *brain slices*

Neocortical slices were prepared as described previously (Hrabětová et al., 2003). Briefly, animals were deeply anesthetized with sodium pentobarbital (50 mg/kg, i. p.), decapitated and the brain was removed from the skull and cooled with ice-cold ACSF. Coronal sections were cut at 400 μm thickness with a vibrating blade microtome (VT 1000 S; Leica Instrument GmbH, Nußloch, Germany), submerged in ACSF and incubated at room temperature for 1-6 hours before measurements. The composition and gassing of the ACSF were the same as described above except that NaCl was 124 mM and KCl was 5 mM.

For measurements, a brain slice was transferred to a submersion tissue chamber (model RC-27L; Warner Instruments, Hamden, CT) perfused at 2.0 ml/min with ACSF warmed to 33 ± 1°C. The chamber was mounted on a Burleigh Gibraltar stage (EXFO Life Sciences, Ontario, Canada) attached to an Olympus BX61WI microscope (Olympus America, Melville, NY).

The RTI- TMA method

Microelectrodes for iontophoretic delivery and TMA^+-ion-selective microelectrodes (ISMs) were both pulled from double-barrelled theta-glass (Cat. No. 64-0811, Warner Instruments) with a final o.d. of 2-5 μm, and fabricated as described by Nicholson (1993). A tetraphenylborate-based ion exchanger (Corning 477317, currently available as IE190 from WPI, Sarasota, FL) was used in the ion-sensing barrel, which was backfilled with 150 mM TMA-chloride. The reference barrel contained 150 mM NaCl. To extract the TMA^+ signal, the voltage measured by the reference barrel was subtracted from the voltage measured by the ion-detecting barrel using a dual-channel microelectrode preamplifier (Model IX2-700; Dagan Corp., Minneapolis, MN). Each ISM was calibrated in solutions containing 0.5, 1, 2, 4, 8 mM TMA-chloride in 150 mM NaCl, using the Nikolsky equation. The iontophoresis microelectrode contained 150 mM TMA^+ chloride.

Diffusion measurements in vivo

The shank of the iontophoretic microelectrode was bent and aligned parallel with the ISM and both were glued together using dental cement with an inter-tip distance of 100-150 μm (Fig. 1A). Control TMA^+ diffusion curves were first recorded in agarose gel (0.3% NuSieve GTG, FMC BioProducts, Rockland, ME, in 150 mM NaCl and 0.5 mM TMA-chloride) to obtain the transport number n_t of the iontophoresis microelectrode and confirm the microelectrode spacing r, then measurements were made in brain to obtain the effective diffusion coefficient D^*, α, λ, and the constant k' that accounted for non-specific loss of TMA^+ from the ECS. A constant bias current of +20 nA was applied to the iontophoresis microelectrode from a high-impedance source (model ION-100, Dagan Corp., Minneapolis, MN) to maintain a stable n_t (Nicholson and Phillips, 1981). To generate a diffusion curve, an additional 100 nA iontophoretic current pulse was applied every 3-5 min for 50 sec. The subtracted ion and reference signals were amplified and low-pass filtered (4 Hz) using a CyberAmp 380 (Axon-CNS, Molecular Devices, Sunnyvale, CA). Diffusion curves were digitized and recorded with a personal computer where they were converted to concentration using the ISM calibration and analyzed with the programs Wanda and Walter (Hrabětová and Nicholson, 2007). The electrode array was aligned along a transverse axis at a depth of 400 μm in the somatosensory neocortex; because the neocortex is isotropic (Lehmenkühler et al. 1993), measurement along a single axis suffices to determine α, λ. and k'.

Diffusion measurement in brain slices

All recordings were made in somatosensory neocortical layers III - VI (Fig. 2A). The methods were similar to those employed *in vivo* with the following changes. The iontophoretic microelectrode and the ISM were held in separate robotic micromanipulators (model MP 285; Sutter Instrument Co., Novato, CA), with each microelectrode at an angle of 31° from the horizontal plane (Fig. 2A) and the two electrode tips advanced into either agarose or cortical slice until they were 200 μm deep and 130 μm apart. The iontophoresis current step varied from 30-100 nA.

Statistical analysis

Values are given as mean ± SEM. Differences between groups were analyzed with a two-sample equal variance *t*-test. Values of $P < 0.05$ were considered significant.

RESULTS

ECS parameters *in vivo*

Fig. 1A shows the experimental arrangement for *in vivo* diffusion measurements. A sequence of diffusion curves recorded in dilute agarose gel and in the somatosensory neocortex of $AQP4^{+/+}$ mice is shown in Fig. 1B. The first set of measurements in agarose gel provided the transport number, n_t, of the iontophoretic microelectrode, and verified the inter-tip distance, *r*, of the micropipette array. Next, the array was positioned in the ACSF flowing above the brain to obtain a recording corresponding to 0.5 mM TMA^+. Then the array was lowered into the brain where, as shown in Fig. 1B, $[TMA^+]_{ECS} > [TMA^+]_{ACSF}$ because the 20 nA bias current applied to the iontophoresis microelectrode continuously released TMA^+ into the ECS. Several diffusion curves were taken in the neocortex and finally, $[TMA^+]_{ACSF}$ was re-verified and records were taken again in agarose. Experiments using $AQP4^{-/-}$ mice were identical.

Fig. 1C shows representative diffusion curves superimposed with fitted theoretical curves for that record. To compare the overall diffusion curves from the two genotypes, we generated theoretical curves (Fig. 1D) based on averaged data (Table 1). The average diffusion curve in $AQP4^{-/-}$ mice had a smaller amplitude than that in $AQP4^{+/+}$ animals, reflecting a larger volume fraction (Fig. 1D *left*). By contrast, scaling the two curves to match amplitudes revealed similar shapes (Fig. 1D *right*) demonstrating similar hindrance to TMA^+ diffusion (tortuosity) in $AQP4^{+/+}$ and $AQP4^{-/-}$ animals.

Altogether, seven $AQP4^{+/+}$ mice and seven $AQP4^{-/-}$ mice were used. In each animal, up to seven diffusion curves were averaged to yield one set of α, λ, and k' per animal and summary values are shown in Fig. 1E and Table 1. These data indicate an enlarged ECS in the neocortex of $AQP4^{-/-}$ mice *in vivo* while the tortuosity was similar in both genotypes.

ECS parameters *in vitro*

The experimental arrangement for *in vitro* diffusion measurements is shown in Fig. 2A. Recordings were taken in the same sequence as described for the *in vivo* preparation.

Representative diffusion curves superimposed with fitted theoretical curves for that record are shown in Fig. 2B. Again, the amplitude of the theoretical diffusion curve (Fig. 2C) based on the mean data (Table 1) was smaller in $AQP4^{-/-}$ than in $AQP4^{+/+}$ mice *in vitro* while the scaled theoretical curves did not differ (Fig. 2C *inset*).

Six brain slices from three $AQP4^{+/+}$ mice and six brain slices from three $AQP4^{-/-}$ mice were used. In each slice, 2-5 diffusion curves were obtained and the parameters averaged to yield

one set of α, λ, and k' per slice with summary values shown in Fig. 2D and Table 1. The *in vitro* results closely resembled those *in vivo*.

DISCUSSION

Using the well-established RTI-TMA method in the somatosensory cortex of AQP4-deficient mice under resting physiological conditions, we found a significant increase of 28% in ECS volume fraction, α, compared to wild type *in vivo* and this was confirmed in brain slices (increase of 21%). There was no difference, however, in ECS tortuosity, λ, between AQP4$^{-/-}$ mice and their WT counterparts. Loss of TMA^{+}, characterized by k', was also unchanged between the two genotypes. Our data enable us to evaluate some of the speculations arising from other recent studies of AQP4$^{-/-}$ mice.

Comparison with other wild-type mouse studies

The RTI-TMA method is the only technique available today for simultaneous measurement of the absolute values of α, λ, and k' *in vivo* as well as *in vitro* (Nicholson and Phillips, 1981; Nicholson 1993). Values of α (0.18 - 0.19), and λ (1.61) found in wild-type mice in the present study can be compared to other *in vivo* studies on wild-type mouse cortex. For ages 3-6 months, Anděrová et al. (2001) found $\alpha = 0.23$, $\lambda = 1.67$; for ages 6-8 months, Syková et al. (2005a) reported $\alpha = 0.20$, $\lambda = 1.47$-1.50; for ages 5-9 months, Syková et al. (2005b) reported $\alpha = 0.17$, $\lambda = 1.57$. Variations among mouse strains probably account for the small differences in values. Loss of TMA^{+} from the ECS *in vivo* in our study was comparable to typical values of $k' = 3\text{-}10 \times 10^{-3}$ (1/sec) in the three studies referenced above and the increased value measured here *in vitro* is likely caused by escape of TMA^{+} at the slice surface (Hrabětová and Nicholson 2007).

Implications of the increased volume fraction in AQP4$^{-/-}$ mice

It has been assumed that the development of the mouse cortex resembles that of the rat (Lehmenkühler et al., 1993) and therefore that α is expanded to about 0.4 in the neonate (Wen et al. 1999). Therefore our results imply that the ECS is reduced to about half this value as the animal matures in both AQP4$^{+/+}$ and AQP4$^{-/-}$ mice, which indicates that AQP4 channels are not obligatory for this contraction.

The increased α in the AQP4-deficient mice compared to wild-type cannot be attributed to a reduction in the volume of the astrocytic endfeet, where the AQP4 channels are most concentrated, because there is no change in endfoot cross-section area in AQP4$^{-/-}$ mice compared to AQP4$^{+/+}$(Manley et al., 2000). Other studies have demonstrated that AQP4 facilitates the removal of excess brain water in models of vasogenic edema where water accumulates in the ECS (Papadopoulos et al., 2004). Thus, it is possible that lack of AQP4 might alter ECS water homeostasis resulting in the expansion of baseline α.

Given that α in AQP4$^{-/-}$ mice was about 28% greater than in AQP4$^{+/+}$ mice, we may ask whether this might have functional consequences, for example in the known increase in seizure threshold (Binder et al. 2004b; Binder et al. 2006). Several *in vitro* studies have shown that application of hyperosmolar solutions containing impermeable substances elevates the seizure threshold in rat hippocampus (Traynelis and Dingledine 1989; Dudek et al. 1990; Pan and Stringer 1996; Kilb et al. 2006). Hyperosmolar solutions should increase α by shrinking cells and Traynelis and Dingledine (1989) confirmed this through impedance measurements. These impedance data (Table 2 in Traynelis & Dingledine, 1989) correspond to a 1-10 % increase in α (assuming α is proportional to impedance). This estimate can be corroborated using the osmotic data of Traynelis & Dingledine (1989) and Equation (13) of Kume-Kick et al. (2002) that predicts a 2-13 % increase in α. Thus, even a moderate expansion of the ECS may

be sufficient to increase the threshold for seizure by reducing the build-up of neuroactive substances in the ECS or decreasing ephaptic interactions that normally promote synchronized firing. Prolonged duration of seizure is more likely related to K^+ clearance because this is impaired in both AQP4$^{-/-}$ (Binder et al. 2006) and α-Syn$^{-/-}$ mice (Amiry-Moghaddam et al. 2003). Such clearance may require water transport or functional coupling of AQP4 and potassium channels (Nagelhus et al. 2004).

Tortuosity is unchanged in AQP4$^{-/-}$ mice

Our finding that tortuosity is unaltered in AQP4$^{-/-}$ mice compared to the wild-type is in contrast to data obtained with fluorescence recovery after photobleaching (FRAP). Using fluorescent dextrans (predominantly 70 kDa), and two FRAP methods, λ was found to be 10-20% less in AQP4$^{-/-}$ mouse neocortex compared to wild-type in undisturbed conditions *in vivo* (Binder et al., 2004a; Papadopoulos and Verkman, 2005; Zador et al., 2008). The 70 kDa dextran molecule is considerably larger than TMA^+ and this might be a factor but further studies with macromolecules will be required to resolve this discrepancy with our results.

Whether or not it is verified that λ is reduced in AQP4$^{-/-}$ mice compared to wild-type when dextrans are employed, the assumption that this implies an increase in α (Binder et al., 2004a; Papadopoulos and Verkman 2005; Zador et al., 2008) is not justified. With the definition of tortuosity employed in the RTI-TMA and FRAP techniques, λ and α are independent parameters (Nicholson and Phillips, 1981; Lehmenkühler et al. 1993; Kume-Kick et al. 2002) and this is borne out by the present data. A dependency may only be derived for some highly constrained models of the ECS (e.g. Tao and Nicholson 2004; Hrabe et al. 2004) and such models do not exist for the complex cytoarchitectonics of the cerebral cortex.

In conclusion, our results show that there is an expansion of the ECS in AQP4$^{-/-}$ mice compared to wild-type; while this probably is inadequate to explain all the differences in pathophysiology seen between these two AQP4 genotypes, the expansion may account for the increased threshold for seizure in AQP4-deficient mice. Furthermore, the data we present here will provide useful parameters for modeling ion and water transport in brain tissue.

ACKNOWLEDGEMENT

This study was supported by the following grants from NIH NINDS: NS050173, NS058931 (to G.M.), NS047557 (to S.H.) and NS28642 (to C.N.). Figure 2A modified with permission from *The Mouse Brain in Stereotaxic Coordinates*, 3rd edition, Keith B.J. Franklin and George Paxinos, Figure 43, 2008, Copyright Elsevier.

REFERENCES

Amiry-Moghaddam M, Williamson A, Palomba M, Eid T, de Lanerolle NC, Nagelhus EA, Adams ME, Froehner SC, Agre P, Ottersen OP. Delayed K^+ clearance associated with aquaporin-4 mislocalization: phenotypic defects in brains of alpha-syntrophin-null mice. Proc Natl Acad Sci U S A 2003;100:13615–13620. [PubMed: 14597704]

Anděrová M, Kubinová S, Mazel T, Chvátal A, Eliasson C, Pekny M, Syková E. Effect of elevated K^+, hypotonic stress, and cortical spreading depression on astrocyte swelling in GFAP-deficient mice. Glia 2001;35:189–203. [PubMed: 11494410]

Binder DK, Papadopoulos MC, Haggie PM, Verkman AS. In vivo measurement of brain extracellular space diffusion by cortical surface photobleaching. J Neurosci 2004a;24:8049–8056. [PubMed: 15371505]

Binder DK, Oshio K, Ma T, Verkman AS, Manley GT. Increased seizure threshold in mice lacking aquaporin-4 water channels. Neuroreport 2004b;15:259–262. [PubMed: 15076748]

Binder DK, Yao X, Zador Z, Sick TJ, Verkman AS, Manley GT. Increased seizure duration and slowed potassium kinetics in mice lacking aquaporin-4 water channels. Glia 2006;53:631–636. [PubMed: 16470808]

Dudek FE, Obenaus A, Tasker JG. Osmolality-induced changes in extracellular volume alter epileptiform bursts independent of chemical synapses in the rat: importance of non-synaptic mechanisms in hippocampal epileptogenesis. Neurosci Lett 1990;120:267–270. [PubMed: 2293114]

Frigeri A, Gropper MA, Umenishi F, Kawashima M, Brown D, Verkman AS. Localization of MIWC and GLIP water channel homologs in neuromuscular, epithelial and glandular tissues. J Cell Sci 1995;108:2993–3002. [PubMed: 8537439]

Hrabe J, Hrabětová S, Segeth K. A model of effective diffusion and tortuosity in the extracellular space of the brain. Biophys J 2004;87:1606–1617. [PubMed: 15345540]

Hrabětová S, Hrabe J, Nicholson C. Dead-space microdomains hinder extracellular diffusion in rat neocortex during ischemia. J Neurosci 2003;23:8351–8359. [PubMed: 12967997]

Hrabětová, S.; Nicholson, C. Biophysical properties of brain extracellular space explored with ion-selective microelectrodes, integrative optical imaging and related techniques. In: Michael, AC.; Borland, LM., editors. Electrochemical Methods for Neuroscience. CRC Press, Taylor Francis Group; Boca Raton: 2007. p. 167-204.

Kilb W, Dierkes PW, Syková E, Vargová L, Luhmann HJ. Hypoosmolar conditions reduce extracellular volume fraction and enhance epileptiform activity in the CA3 region of the immature rat hippocampus. J Neurosci Res 2006;84:119–129. [PubMed: 16634058]

Kume-Kick J, Mazel T, Vořišek I, Hrabětová S, Tao L, Nicholson C. Independence of extracellular tortuosity and volume fraction during osmotic challenge in rat neocortex. J Physiol 2002;542:515–527. [PubMed: 12122149]

Lehmenkühler A, Syková E, Svoboda J, Zilles K, Nicholson C. Extracellular space parameters in the rat neocortex and subcortical white matter during postnatal development determined by diffusion analysis. Neuroscience 1993;55:339–351. [PubMed: 8377929]

Ma T, Yang B, Gillespie A, Carlson EJ, Epstein CJ, Verkman AS. Generation and phenotype of a transgenic knockout mouse lacking the mercurial-insensitive water channel aquaporin-4. J Clin Invest 1997;100:957–962. [PubMed: 9276712]

Manley GT, Fujimura M, Ma T, Noshita N, Filiz F, Bollen AW, Chan P, Verkman AS. Aquaporin-4 deletion in mice reduces brain edema after acute water intoxication and ischemic stroke. Nature Medicine 2000;6:159–163.

Manley GT, Binder DK, Papadopoulos MC, Verkman AS. New insights into water transport and edema in the central nervous system from phenotype analysis of aquaporin-4 null mice. Neuroscience 2004;129:983–991. [PubMed: 15561413]

Nagelhus EA, Mathiisen TM, Ottersen OP. Aquaporin-4 in the central nervous system: cellular and subcellular distribution and coexpression with KIR4.1. Neuroscience 2004;129:905–913. [PubMed: 15561407]

Nicholson C, Phillips JM. Ion diffusion modified by tortuosity and volume fraction in the extracellular microenvironment of the rat cerebellum. J Physiol 1981;321:225–257. [PubMed: 7338810]

Nicholson C. Ion-selective microelectrodes and diffusion measurements as tools to explore the brain cell microenvironment. J Neurosci Meth 1993;48:199–213.

Nielsen S, Nagelhus EA, Amiry-Moghaddam M, Bourque C, Agre P, Ottersen OP. Specialized membrane domains for water transport in glial cells: high-resolution immunogold cytochemistry of aquaporin-4 in rat brain. J Neurosci 1997;17:171–180. [PubMed: 8987746]

Pan E, Stringer JL. Influence of osmolality on seizure amplitude and propagation in the rat dentate gyrus. Neurosci Lett 1996;207:9–12. [PubMed: 8710214]

Papadopoulos MC, Manley GT, Krishna S, Verkman AS. Aquaporin 4 facilitates the reabsorption of excess fluid in vasogenic brain edema. FASEB J 2004;18:1291–1293. [PubMed: 15208268]

Papadopoulos MC, Verkman AS. Aquaporin-4 gene disruption in mice reduces brain swelling and mortality in pneumococcal meningitis. J Biol Chem 2005;280:13906–13912. [PubMed: 15695511]

Syková E, Vořišek I, Antonova T, Mazel T, Meyer-Luehmann M, Jucker M, Hájek M, Or M, Bureš J. Changes in extracellular space size and geometry in APP23 transgenic mice: A model of Alzheimer's disease. Proc Natl Acad Sci U S A 2005a;102:479–484. [PubMed: 15630088]

Syková E, Vořišek I, Mazel T, Antonova T, Schachner M. Reduced extracellular space in the brain of tenascin-R- and HNK-1-sulphotransferase deficient mice. Eur J Neurosci 2005b;22:1873–1880. [PubMed: 16262627]

Tao L, Nicholson C. Maximum geometrical hindrance to diffusion in brain extracellular space surrounding uniformly spaced convex cells. J Theoret Biol 2004;229:59–68. [PubMed: 15178185]

Traynelis SF, Dingledine R. Role of extracellular space in hyperosmotic suppression of potassium-induced electrographic seizures. J Neurophysiol 1989;61:927–938. [PubMed: 2723735]

Wen H, Nagelhus EA, Amiry-Moghaddam M, Agre P, Ottersen OP, Nielsen S. Ontogeny of water transport in rat brain: postnatal expression of the aquaporin-4 water channel. Eur J Neurosci 1999;11:935–945. [PubMed: 10103087]

Zador Z, Magzoub M, Jin S, Manley GT, Papadopoulos MC, Verkman AS. Microfiberoptic fluorescence photobleaching reveals size-dependent macromolecule diffusion in extracellular space deep in brain. Faseb J 2008;22:870–879. [PubMed: 17965267]

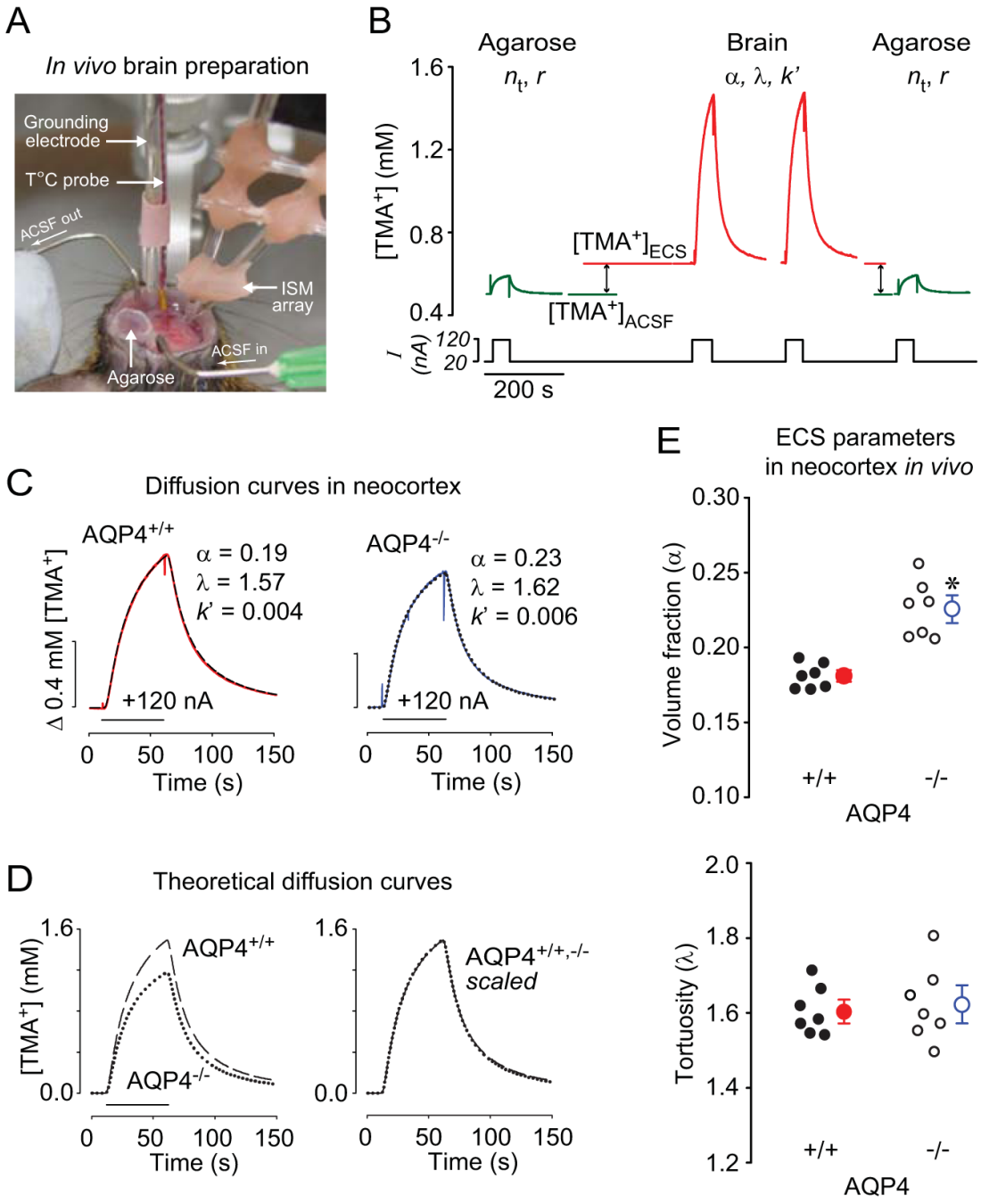

Figure 1.

Diffusion of TMA^+ in the somatosensory neocortex of $AQP4^{+/+}$ and $AQP4^{-/-}$ mice *in vivo*. **A.** Photograph of recording arrangement for RTI-TMA diffusion measurements. The mouse head was immobilized in a stereotaxic frame. A micromanipulator positioned the microelectrodes that were glued with dental cement into an array with fixed inter-tip distance. The grounding electrode and the temperature probe were positioned nearby. See *Material and Methods* for details. **B.** Sequence of diffusion curves recorded in dilute agarose gel and neocortex of $AQP4^{+/+}$ mice. Several records were obtained in agarose before and after brain measurements. See *Results* section for details. **C.** Examples of TMA^+ diffusion curves in $AQP4^{+/+}$ and $AQP4^{-/-}$ mice. The measurements were done at 37°C where $D_{37} = 1.31 \times 10^{-5}$

cm^2/sec. TMA^+ pulse was applied for 50 sec (*horizontal bar*), *r* was 144 μm and 124 μm for $AQP4^{+/+}$ and $AQP4^{-/-}$, respectively, and n_t was 0.33 for both records. Recorded curves (*red and blue*) are superimposed with corresponding theoretical curves obtained from fitting procedure (*dashed and dotted*). **D.** Diffusion curves obtained in $AQP4^{+/+}$ compared with those in $AQP4^{-/-}$ mice by generating theoretical curves based on the average α, λ, and *k*' values (Table 1 *and Panel E*) with the following parameters: temperature 37°C, bias current +20 nA, main current +120 nA for 50 s, $r = 130$ μm, $n_t = 0.4$. The $AQP4^{-/-}$ theoretical curve had smaller amplitude than that for $AQP4^{+/+}$ animals (*left*) reflecting a larger α but both curves had similar shapes (*right*) indicating similar values of λ. **E.** Scatter plots of whole data sets. Each small circle represents the average from one animal. Large circles are mean ± SEM values; *P < 0.001.

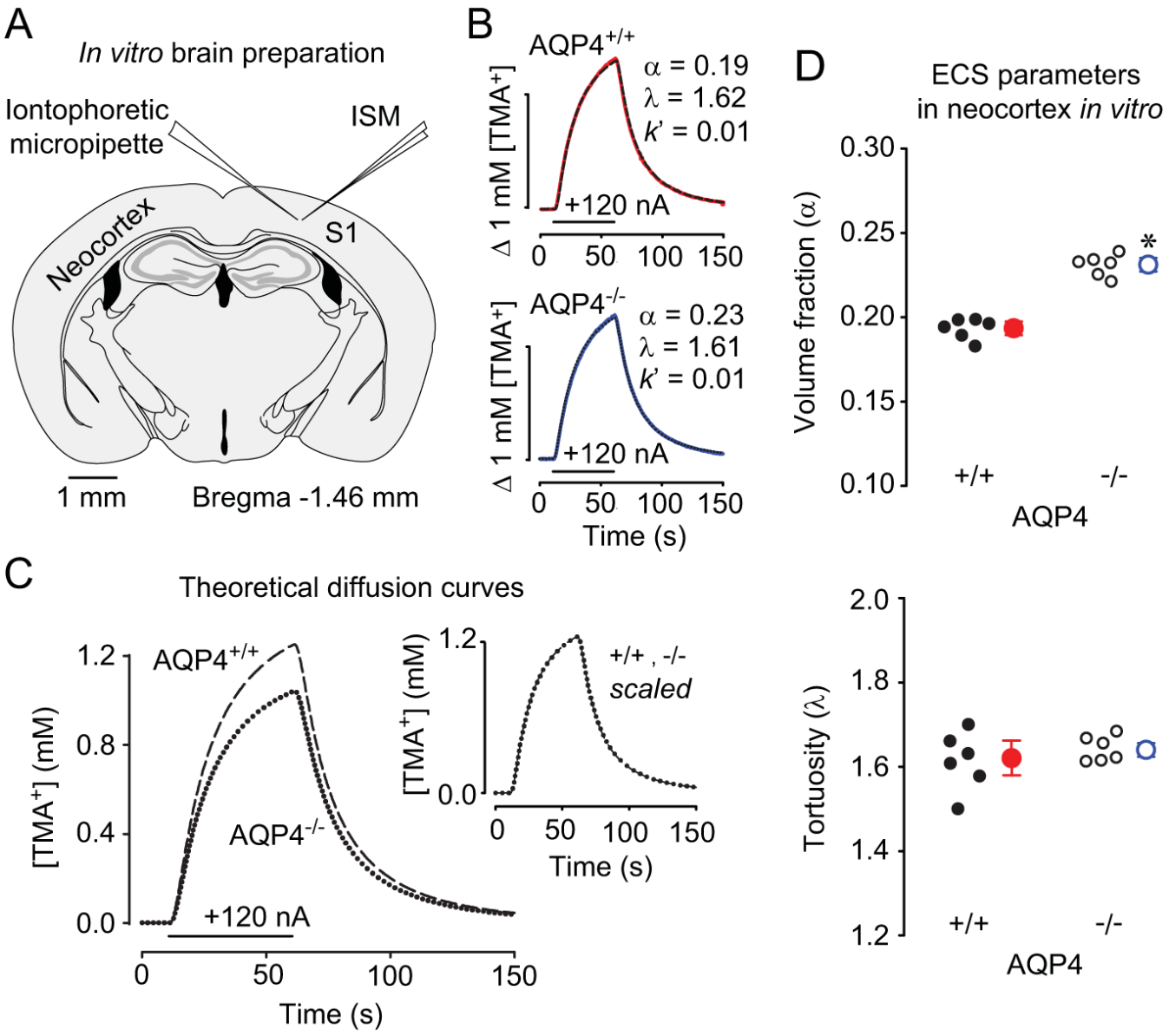

Figure 2.

Diffusion of TMA^+ in the somatosensory neocortex (*S1*) of $AQP4^{+/+}$ and $AQP4^{-/-}$ mice *in vitro*. **A.** A schematic of coronal brain slice with two independent microelectrodes positioned in *S1*. **B.** Representative TMA^+ diffusion curves in $AQP4^{+/+}$ (*top*) and $AQP4^{-/-}$ (*bottom*) mice. The measurements were done at 34°C and 32°C in $AQP4^{+/+}$ and $AQP4^{-/-}$ mice respectively; $D_{34} = 1.24 \times 10^{-5}$ cm^2/sec and $D_{32} = 1.19 \times 10^{-5}$ cm^2/sec. TMA^+ pulse was applied for 50 sec (*horizontal bar*), *r* was 130 μm, and n_t was 0.39 and 0.48 for $AQP4^{+/+}$ and $AQP4^{-/-}$ mice, respectively. Actual $AQP4^{+/+}$ record was taken with 60 nA current but scaled to 120 nA for consistency. In both panels, recorded curves (*solid red or blue lines*) are superimposed with corresponding theoretical curves obtained from fitting procedure (*dashed* and *dotted*). **C.** As in Fig. 1, to compare the diffusion properties in $AQP4^{+/+}$ and $AQP4^{-/-}$ mice, two theoretical curves were generated from average *α*, *λ*, and *k*' values (Table 1 *and Panel D*) with the same parameters as in Fig. 1. except temperature 34°C. As in Fig. 1, TMA^+ diffusion curve in $AQP4^{-/-}$ mice has smaller amplitude than $AQP4^{+/+}$ but similar shape (*inset*). **D.** Scatter plots

of entire data sets showing a significant increase in the volume fraction in $AQP4^{-/-}$ (*top*) but no change in the tortuosity (*bottom*). Each small circle represents the average from a single slice. Large circles are mean ± SEM values; $*P < 0.001$.

Table 1

Extracellular volume fraction, tortuosity, and TMA^+ loss in the somatosensory neocortex of $AQP4^{+/+}$ and $AQP4^{-/-}$ mice

Genotype	Preparation	*α*	*λ*	*k' (1/sec)*	*n*
$AQP4^{+/+}$	*in vivo*	0.18 ± 0.003	1.61 ± 0.02	0.0031 ± 0.0009	7
$AQP4^{-/-}$		0.23 ± 0.007*	1.62 ± 0.04	0.0045 ± 0.0001	7
$AQP4^{+/+}$	*in vitro*	0.19 ± 0.002	1.61 ± 0.03	0.013 ± 0.001	6
$AQP4^{-/-}$		0.23 ± 0.003*	1.64 ± 0.01	0.013 ± 0.001	6

Data are expressed as mean ± SEM

n is number of animals (*in vivo*) or brain slices (*in vitro*)

* statistically significant difference ($P < 0.001$, two-sample equal variance *t*-test) between $AQP4^{+/+}$ and $AQP4^{-/-}$